Femtosecond frequency comb based distance measurement in air

Balling, P.; Kren, P.; Masika, P.; van den Berg, S.A.

published in
Optics Express
2009

DOI (link to publisher)
10.1364/OE.17.009300

document version
Publisher's PDF, also known as Version of record

Femtosecond frequency comb based distance measurement in air

Petr Balling,[1,*] Petr Křen,[1] Pavel Mašika,[1] and S.A. van den Berg[2]

[1]*Czech Metrology Institute, Laboratories of Fundamental Metrology, V Botanice 4, 150 72 Prague, Czech Republic*
[2]*VSL, Thijsseweg 11, 2629 JA Delft, The Netherlands*
[*]*Corresponding author: pballing@cmi.cz*

Abstract: Interferometric measurement of distance using a femtosecond frequency comb is demonstrated and compared with a counting interferometer displacement measurement. A numerical model of pulse propagation in air is developed and the results are compared with experimental data for short distances. The relative agreement for distance measurement in known laboratory conditions is better than 10^{-7}. According to the model, similar precision seems feasible even for long-distance measurement in air if conditions are sufficiently known. It is demonstrated that the relative width of the interferogram envelope even decreases with the measured length, and a fringe contrast higher than 90% could be obtained for kilometer distances in air, if optimal spectral width for that length and wavelength is used. The possibility of comb radiation delivery to the interferometer by an optical fiber is shown by model and experiment, which is important from a practical point of view.

OCIS codes: (120.0120) Instrumentation, measurement, and metrology; (010.3310) Laser beam transmission; (120.3180) Interferometry; (010.1300) Atmospheric propagation; (260.2030) Dispersion; (120.3940) Metrology.

References and links

1. For a general review see, e.g., S. T. Cundiff and J. Ye, "Colloquium: Femtosecond optical frequency combs," Rev. Mod. Phys. **75**, 325–342 (2003).
2. P. Gill, "Optical frequency standards," Metrologia **42**, S125–S137 (2005).
3. L. Hollberg, S. Diddams, A. Bartels, T. Fortier, and K. Kim, "The measurement of optical frequencies," Metrologia **42,** S105–S124 (2005).
4. E. V. Baklanov and A. K. Dmitriev, "Absolute length measurements with a femtosecond laser," Quantum Electron. **32,** 925–928 (2002).
5. J. Ye, "Absolute measurement of a long, arbitrary distance to less than an optical fringe," Opt. Lett. **29**, 1153–1155 (2004), http://www.opticsinfobase.org/abstract.cfm?URI=ol-29-10-1153.
6. K.-N. Joo, Y. Kim, and S.-W. Kim, "Distance measurements by combined method based on a femtosecond pulse laser," Opt. Express **16**, 19799–19806 (2008), http://www.opticsinfobase.org/abstract.cfm?URI=oe-16-24-19799.
7. Y. Salvadé, N. Schuhler, S. Lévêque, and S. Le Floch, "High-accuracy absolute distance measurement using frequency comb referenced multiwavelength source," Appl. Opt. **47**, 2715–2720 (2008), http://www.opticsinfobase.org/ao/abstract.cfm?URI=ao-47-14-2715.
8. M. Cui, R. N. Schouten, N. Bhattacharya, and S. A. van den Berg, "Experimental demonstration of distance measurement with a femtosecond frequency comb laser," J. Eur. Opt. Soc. Rapid Publ. **3,** 08003 (2008), https://www.jeos.org/index.php/jeos_rp/article/view/08003/246.
9. K. Minoshima, T. R. Schibli, H. Inaba, Y. Bitou, F.-L. Hong, A. Onae, H. Matsumoto, Y. Iino, and K. Kumagai, "Ultrahigh dynamic-range length metrology using optical frequency combs," NMIJ-BIPM Joint Workshop on Optical Frequency Comb, Tsukuba, (2007), http://www.nmij.jp/~nmijclub/photo/docimgs/minoshima_2007May_web2.pdf .
10. J. Zhang, Z. H. Lu, and L. J. Wang, "Precision measurement of the refractive index of carbon dioxide with a frequency comb," Opt. Lett. **32**, 3212–3214 (2007), http://www.opticsinfobase.org/abstract.cfm?URI=ol-32-21-3212
11. Ciddor formula for refractive index of air, http://emtoolbox.nist.gov/Wavelength/Documentation.asp.
12. J. E. Decker and J. R. Pekelsky, "Uncertainty evaluation for the measurement of gauge blocks by optical interferometry," Metrologia **34**, 479–493 (1997).

#108459 - $15.00 USD Received 10 Mar 2009; revised 17 Apr 2009; accepted 18 Apr 2009; published 19 May 2009

13. Y. Yamaoka, L. Zeng, K. Minoshima, and H. Matsumoto, "Measurements and numerical analysis for femtosecond pulse deformations after propagation of hundreds of meters in air with water-vapor absorption lines," Appl. Opt. **43**, 5523–5530 (2004).
14. P. Balling and P. Kren, "Absolute frequency measurements of wavelength standards 532 nm, 543 nm, 633 nm, and 1540 nm," Eur. Phys. J. D **48**, 3–10 (2008).
15. Y. Yamaoka, K. Minoshima, and H. Matsumoto, "Direct measurement of the group refractive index of air with interferometry between adjacent femtosecond pulses," Appl. Opt. **41**, 4318–4324 (2002).
16. J.-P. Wallerand, A. Abou-Zeid, T. Badr, P. Balling, J. Jokela, R. Kugler, M. Matus, M. Merimaa, M. Poutanen, E. Prieto, S. van den Berg, and M. Zucco, "Towards new absolute long-distance measurement in air," 2008 NCSL International Workshop and Symposium, Orlando (USA), http://www.longdistanceproject.eu/files/towards_new_absolute.pdf.

1. Introduction

The invention of the optical frequency comb is of key importance in fields like optical spectroscopy, ultrashort pulse generation, optical clocks, and for calibration of optical frequency standards [1–3]. A frequency comb that is referenced to a time standard also enables direct transfer of the precisely known repetition frequency of length, according to the SI definition of the meter. Several methods for length measurement with a frequency comb have been proposed: using a perfect Fabry–Perot interferometer [4]; using a combination of time-of-flight measurement and fringe-resolved interferometry [5]; using a combination of spectrally resolved interferometry, synthetic wavelength interferometry, and time-of-flight measurements [6]; or using multiple wavelength interferometry with several cw lasers referenced to a frequency comb [7]. The application of frequency combs for distance measurement in air has been demonstrated for a short distance [8]. In this application the frequency comb can be considered as a source for multiwavelength interferometry with a synthetic wavelength corresponding to the repetition frequency. Another approach is to detect the high harmonics of the repetition rate and derive the distance from a measurement of the phase shift of the returning radiation. This approach has been used for several years by Minoshima *et al.* [9], where an agreement with a laser interferometer during one week to better than 0.1 ppm is reported. The interferometric measurement with frequency comb radiation was also used for precise measurement of the refractive index of air and other gasses in a stabilized cavity [10].

When measuring in air, the dispersion influence has to be taken into account because it affects the distance between consecutive pulses (group velocity differs from phase velocity). Moreover, the pulses are elongated due to group velocity dispersion, which leads to a decrease of peak power.

A model for ultrashort pulse propagation in air for various pulse central wavelengths, spectral shapes, and atmospheric conditions is presented in this paper. The influence of dispersion is evaluated and the method for minimizing broadening by using appropriate spectral width is shown. Experimental results of measurements of distances up to 1.5 m with a frequency comb are compared with the results of a counting interferometer. The detected interference patterns for various spectral shapes (fs laser settings) and various distances are compared with the model.

Several different methods of interferogram position detection are proposed and compared: first, the detection of interferogram envelope characteristics (peak position, center of gravity) and second, the evaluation of a stationary phase point for one or several wavelengths. The first method seems promising for long-distance measurement, where the detected fringes are expected to be distorted by the instability of the optical length to be measured, by fast changes in wavefront distortion, and by the instability (limited coherence length) of the frequency comb. The phase-detection method was proved to be useful for short distance measurement in laboratory conditions.

2. Principle of interferometric distance measurement with a frequency comb

In a phase-locked frequency comb laser, the phase relation between subsequent pulses is conserved, which allows for interferometry between different pulses. The pulse train may be

#108459 - $15.00 USD Received 10 Mar 2009; revised 17 Apr 2009; accepted 18 Apr 2009; published 19 May 2009

sent into an interferometer, as shown in Fig. 1. When the path length difference of the interferometer arms is a multiple of the interpulse distance l_{pp}, an interferogram (cross-correlation function) can be measured. In order to accomplish spatial overlap between the pulses traveling in the long and short arms, respectively, the short arm can be adjusted within the range $l_{pp}/2$.

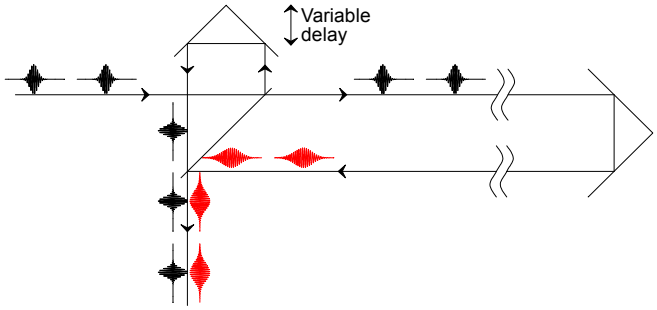

Fig. 1. Schematic representation of the setup for interferometric distance measurement with a frequency comb.

A frequency comb usually has a repetition rate f_r of 100–1000 MHz, which leads to an interpulse distance $l_{pp}=c_o/(n_{ge} f_r)$ of 30–300 cm. Here c_o is the speed of light in vacuum and n_{ge} is the effective group refractive index of air. The range of non-ambiguity of the distance measurement is determined by l_{pp}. An initial measurement with this accuracy can be done easily with other methods, or the integer number N of l_{pp} in a measured distance can be estimated by change of f_r and the measurement of a corresponding shift of the interferogram, if the relative precision of the shift measurement is better then $1/N$. Thus the path length difference in the interferometer is measured as a multiple of the interpulse distance and is retrieved from the center of the measured interferogram. This measurement principle can be applied for absolute distance measurements by placing the measuring reflector to the zero position (of baseline) and adjusting the reference arm for coherence maximum, then moving the measuring reflector to the target point of the long arm and adjusting the short arm to obtain a coherence maximum again. The displacement of the short arm may be measured, e.g., by an auxiliary counting interferometer or a calibrated line scale. There is no need for continuous measurement while moving the reflector (in contrast to counting the interferometer displacement measurement). By scanning the reference arm around the coherence maxima position, an interferogram is obtained. The interferogram can be measured as either first- or second-order correlation functions. The shape of the interferogram depends on the spectral content and the fact that the pulses experience different dispersions in the long and short arms. For second-order correlation, the chirp of the initial pulse comes into play. To obtain an accurate distance measurement, the interpulse distance l_{pp} needs to be known accurately and thus the effective group refractive index of air.

3. Numerical model of comb pulse propagation in air

The group velocity v_g or the group refractive index n_g can be calculated analytically as

$$v_g = \frac{\partial \omega}{\partial k}, \tag{1}$$

$$n_g = \frac{c}{v_g} = n + f\frac{\partial n}{\partial f} = n - \lambda_c \frac{\partial n}{\partial \lambda} \cong n + f_c \frac{n(f_c + f_r) - n(f_c - f_r)}{2 f_r}, \tag{2}$$

where λ_c and f_c are the central wavelength and frequency of the pulse spectra, respectively, and n is corresponding phase refractive index.

Equations (1) and (2) are valid only for linear dispersion; for a broader spectral range (ultrashort pulses) some kind of spectral averaging is needed. Moreover, the derivative $\partial n/\partial f$

#108459 - $15.00 USD Received 10 Mar 2009; revised 17 Apr 2009; accepted 18 Apr 2009; published 19 May 2009

leads to a relatively complicated expression when using precise refractive index formulas such as Ciddor's [11]. These are the reasons for creating a numerical model that enables efficient calculation of mean group refractive indices for different spectral shapes and shows the shape of the interferogram for a certain distance.

We have implemented a model based on plane wave propagation, describing the total field at position x_n as

$$E(x_n) = \sum_i E_i \cos k_i x_n \cdot \tag{3}$$

Here $k_i = 2\pi\, n_i f_i / c_o$ represents the angular wavenumber in air and E_i is the (relative) electric field of the frequency comb component i. The frequency f_i is given by: $f_i = f_o + i f_r$, with f_o as the carrier-envelope offset frequency. For each frequency f_i the phase refractive index n_i is taken into account, which is calculated using the Ciddor formula [11] or the modified Edlen formula [12]. The atmospheric conditions—air pressure, temperature, humidity and CO_2 content—are provided as input. The input pulse properties can be set by specifying f_r and f_o as the central wavelength and the spectral width and shape. Alternatively, an arbitrary (measured) spectral shape can be loaded. For the individual comb components, the relative electric field and the phase index are calculated. From these results the group refractive index for the central wavelength and the mean group refractive index (spectrally weighted according to light intensity) are determined. For the latter, Eq. (2) (with f_i instead of f_c) is applied for calculation of the contribution of each spectral component to the effective group index.

For a user-given distance to be measured, there are two ways of obtaining an interferogram: either the adjustment of the reference arm length or the adjustment of f_r. In both cases these values are chosen such that the path length difference between measuring and the reference arm equals an integer multiple of l_{pp}. Once the expected position of interferogram "center" is known, a local value of the electric field (at time =0) is calculated as a sum of the contributions of all comb components according to Eq. (3). Both $E_r(x_n)$ for the reference pulse (x_n around zero) and $E_m(x_n)$ for the measuring pulse (with x_n around the expected path length difference) are determined, each of them in N points (with n ranging from $-N/2$ to $N/2$). We have prepared the spatial profile of the electric field of reference and the measuring pulses (strictly speaking, an instant picture of a profile in time equal to the integer multiple of femtosecond laser periods $1/f_r$). The (relative) interferogram $I(x)$, i.e., the time-averaged light intensity variation with changing the path length, is obtained from the convolution of the electric fields of both pulses as

$$I_d = \sum_{n=-N/2}^{N/2} \left(E_r(x_n) + E_m(x_{n+d})\right)^2 \tag{4}$$

for each displacement index d. The convolution is calculated numerically; if index $n+d$ is outside the interval $-N/2$ to $N/2$, the E_m is taken equal to zero. The range of x is chosen such that both E_r and E_m pulses fully fit into the range of calculated path lengths—only negligible tails were outside—and N is chosen such that the increment of the position is much smaller than the central wavelength.

The nonlinear (second order) interferogram is calculated similarly from

$$I_d^2 = \sum_{n=-N/2}^{N/2} \left(E_r(x_n) + E_m(x_{n+d})\right)^4 \cdot \tag{5}$$

Figure 2 shows an example of calculation for a Gaussian pulse (central wavelength 800 nm, width 40 THz), 2 m path (1 m distance), 100 kPa, 20°C, 50% rel. humidity, and 400 ppm of CO_2. It is observed that air dispersion is significant even for this short distance; the measuring pulse returns stretched (the red curve in the middle picture compared to the green one) and the contrast of the linear interferogram is decreased by a few percent.

#108459 - $15.00 USD Received 10 Mar 2009; revised 17 Apr 2009; accepted 18 Apr 2009; published 19 May 2009

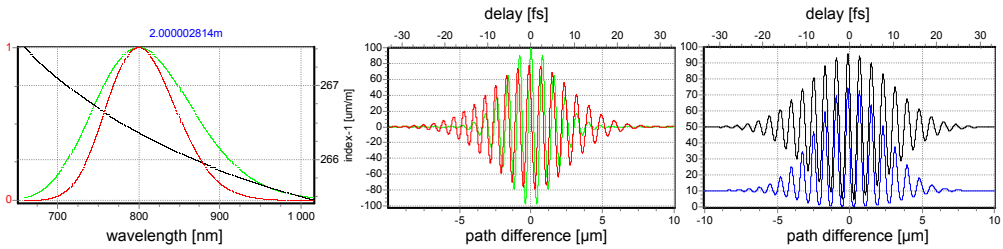

Fig. 2. Typical model results. Left chart, relative spectra (red, light intensity; green, electric field intensity) and dispersion (black, right axis). Middle chart, electric fields of reference and measuring pulses. Right chart, linear (black) and second-order (blue) interferogram in percents relative to intensity of interferogram of the reference pulse with itself.

The interference patterns in Fig. 2 are calculated for an ideally coherent (no chirp) pulse entering the interferometer (the green curve in the middle chart) and for no additional dispersion in the interferometer except for dispersion in air. However, the model also allows for evaluating the influence of the dispersion before the interferometer (glass windows, lenses, filters, dead path in air—common to both interferometer arms) or in one of its arms.

The spectral modulation of the radiation exiting the comb interferometer is also evaluated. In an ideal case all wavelengths from the fs laser spectra are mode locked—they have the same phase at the peak of the pulse envelope. Also, the phase difference between the radiation of the reference arm and of the measuring arm is the same for all wavelengths when the arm path difference is close to zero and if there is no dispersion difference between arms (all wavelengths interfere constructively for displacement corresponding to light fringe position or destructively for dark fringe). In a non-dispersive environment this is valid also for displacements close to integer multiples of l_{pp}. However, due to air dispersion, the coherence is maintained only for some part of the spectra for path length difference L equal to non-zero multiples of l_{pp}. The light intensity for a certain value of λ is given by

$$I(\lambda_i, L) = 2E_i^{\,2}\left(1+\cos k_i L\right). \tag{6}$$

Concerning the time needed for processing, it could be considerably long, e.g., for f_r = 200 MHz, total width of the evaluated spectra 160 THz and for 20 nm steps over the range ±0.1 mm, all 800 000 of the comb components have to be evaluated for each 10 000 position points, i.e., 2×10^9 of cosine evaluations and a few multiplications (with extended precision) have to be done for E field profiles (which take 18 min on a PC with an x86 2 GHz processor). But, the resulting position and shape of the interferogram is the same if a higher f_r is chosen (equal to an integer multiple of the original value) as long as the remaining number of components is sufficient for a detailed representation of incident radiation spectra. So to save time, the above described calculation can be done for f_r = *20* GHz (8 000 components) in just 12 seconds. But if a detailed spectral shape including, e.g., molecular absorption spectral lines is needed [13], a full set of wavelength components (real values of f_r and f_o) is needed.

The model is created in a Borland Turbo Delphi environment. The executable program for MS Windows can be obtained for free via the corresponding author's e-mail.

4. Results of modeling

The position of the center of gravity of squares of the electric field profile calculated using Eq. (3) is in excellent agreement with the position predicted by the mean group refractive index for both symmetrical and asymmetrical input spectra (e.g., below 10^{-10} relative for 100 m distance). For symmetrical spectra the agreement is even much better.

Any dispersion that is common to both arms—before or inside the interferometer—does not affect the linear interferogram (it makes the E field pulses longer in time, the peak intensity weaker, and the spatial positions of electric field envelopes in t = 0 are shifted, but

#108459 - $15.00 USD Received 10 Mar 2009; revised 17 Apr 2009; accepted 18 Apr 2009; published 19 May 2009

their convolution remains spectral transform-limited and l_{pp} remains constant). Only the second-order interferogram background shows the real pulse length, as can be seen in Fig. 3.

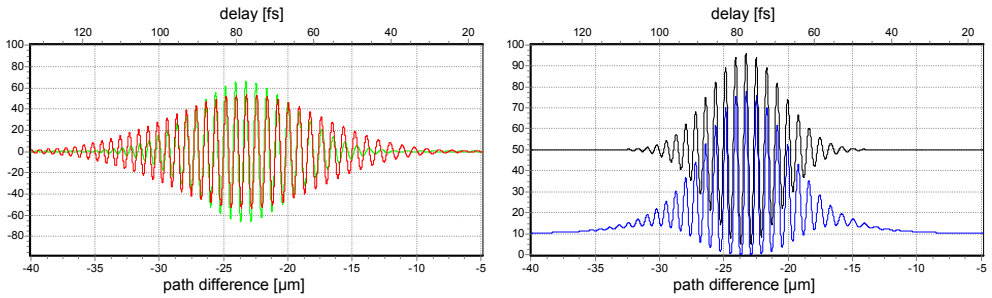

Fig. 3. Modeled E fields (left) and interferograms (right) for the same condition as in Fig. 2 but with linear chirp -10 μm/160 THz. The horizontal scale range is doubled compared to Fig. 2. The centers of envelopes of each pulse of the train are shifted by -23 μm due to this chirp. The black curve (first-order interferogram) is exactly the same as in Fig. 2.

This feature is important because it relaxes the requirements to measurement setup for linear interferogram detection—in that case even a long (dispersive) optical fiber could be used before the interferometer.

For short distance measurement it is advantageous to use a broad spectral range—the linear interferogram is short (not affected by any chirp/dispersion, which is common for measuring and reference pulses). However, for a very long distance (high dispersion in the measuring arm) the broader the spectra, the longer the interferogram and the lower its contrast. So for each distance to be measured there is an optimal spectral band giving both the shortest interferogram and the high contrast (only single frequency gives 100% contrast in a dispersive environment for any distance). Spectral modulation analysis is useful for easily finding these optimal spectral bands. For given input spectra and distance, first n_{ge} and l_{pp} are calculated (the f_r or reference arm length is changed such that the path difference equals an integer multiple of l_{pp}). The spectral modulation curve at that position shows spectral bands (Fig. 4) for which coherence is maintained—the broadest one in the center is the optimal one.

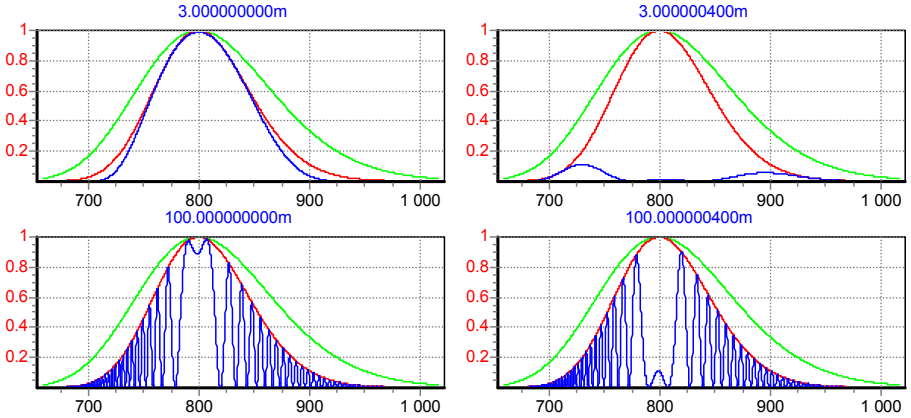

Fig. 4. Spectral modulation of ~800 nm radiation due to interference after the measuring pulse has passed different path lengths in air. All plots are for fringes in the very center of the interferogram. Red original (input) spectra, blue modulated spectra, horizontal scale wavelength in nanometers. Top, 1.5 m distance; bottom, 50 m distance; left, light fringe; right, dark fringe.

It may not be easy to get a filter producing Gaussian spectra, so we have evaluated the effect of rectangular spectral filters. Of course, neither the resulting E field profile nor the interferogram envelope are Gaussian anymore—there appear many side lobes—but for

#108459 - $15.00 USD Received 10 Mar 2009; revised 17 Apr 2009; accepted 18 Apr 2009; published 19 May 2009

optimal filter width, the central part of the interferogram is clearly perceptible and has over 90% contrast (Fig. 5).

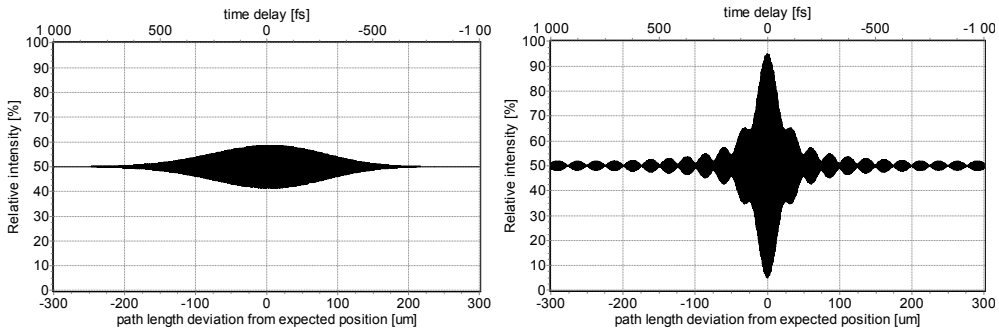

Fig. 5. Modeled interferograms for the same condition as in Fig. 2 and path length difference 100 m (distance 50 m). Left, full spectra; right, after "optimal" rectangular filter ±13.0 nm.

Table 1 contains the optimal widths of rectangular spectral filters for central wavelengths 400 nm, 800 nm, and 1550 nm and for several distances from 1.5 m to 1 km. In the last three columns there is the half width of the central part of the interferogram envelope expressed as the path length change from the center (in micrometers) or relatively to the path traveled in air by the measuring pulse or as the number of fringes of the wavelength used. Table 1 shows that the relative width of the optimal interferogram decreases with the increasing distance.

Table 1. Optimal Filter Widths for Different Central Wavelengths and Distances

Central wl./fr.		Path in air	Distance	Opt. filter for >90% contrast		HWHM length of interferogram		
nm	THz	m	m	nm	THz	μm	ppm	fringes
400	749	3	1.5	±11.0	±20.6	4.5	1.5	11
		30	15	±4.0	±7.5	14	0.5	35
		100	50	±2.2	±4.1	26	0.26	65
		300	150	±1.2	±2.2	47	0.16	118
		1000	500	±0.65	±1.2	90	0.09	225
		2000	1000	±0.5	±0.8	140	0.07	350
800	375	3	1.5	±70.0	±32.8	3	1	4
		30	15	±22.0	±10.3	9	0.3	11
		100	50	±13.0	±6.1	17	0.17	21
		300	150	±8.0	±3.7	28	0.09	35
		1000	500	±4.5	±2.1	50	0.05	63
		2000	1000	±3.0	±1.4	75	0.04	94
1550	193	3	1.5	±350.0	±43.7	2.5	0.83	2
		30	15	±130	±16.2	7	0.23	5
		100	50	±70	±8.7	13	0.13	8
		300	150	±40	±5.0	22	0.07	14
		1000	500	±22	±2.7	40	0.04	26
		2000	1000	±16	±2.0	52	0.026	34

In order to simplify the uncertainty estimation, we have calculated the sensitivity coefficients of the mean group refractive index of air on a variation of atmospheric conditions for several mean wavelengths in the vicinity of 100 kPa, 20°C, 50% RelH, 400 ppm, and the Gaussian spectral profile of width 40 THz (Table 2). The coefficients do not differ much from those of phase refractive indices.

#108459 - $15.00 USD Received 10 Mar 2009; revised 17 Apr 2009; accepted 18 Apr 2009; published 19 May 2009

Table 2. Sensitivity Coefficients of Mean Group Refractive Index on Central Wavelength and on Environment Parameters[a]

	n_{ge} sensitivity coefficient [ppb]				variation for 5×10^{-8} rel. change			
	400nm	800nm	1550nm		400nm	800nm	1550nm	
central wavelength	-163.23	-17.85	-2.41	per nm	-0.27	-2.51	-18.55	nm
air pressure	2.95	2.72	2.66	per Pa	15.14	16.46	16.79	Pa
air temperature	-1027.26	-950.82	-933.94	per °C	-43.5	-47.0	-47.9	mK
relative humidity	-6.93	-8.26	-8.62	per %	-6.45	-5.41	-5.19	%
CO_2 content	0.16	0.14	0.14	per ppm	287	312	318	ppm

[a]In the right part, variation of these parameters causing change of mean group refractive index of 5×10^{-8} relative change.

A frequency comb from an infrared fiber mode-locked laser is particularly favorable due to low dispersion and also due to easier transportation and use as well as eye safety. The typically lower f_r is a disadvantage, bringing longer l_{pp}—a longer movement of the reference arm for finding the interferogram. This problem could be solved by folding the beam on the moving stage (or by measuring distances only close to the integer multiple of $l_{pp}/2$ (close enough such that an adjustment of l_{pp} by f_r is possible).

It should be noted that in principle it is possible to obtain a very narrow (transform-limited) interferogram envelope for any distance simply by introducing the same dispersion into the reference arm, as it is due to air in the measuring arm—but this dispersion would need to be known with precision, given by target uncertainty of the distance measurement.

5. Experimental setup and measurement procedure

The experimental arrangement for the evaluation of distance measurement with a comb is shown in Fig. 6. We use a Ti:sapphire femtosecond frequency comb from Menlo Systems FC 8004 dedicated primarily to measurement of optical frequencies [14]. The repetition rate of the fs laser is about 200 MHz (known better than 2.5×10^{-11} rel. for 1 s averages, k=2) and the cavity length is approximately 0.75 m (l_{pp}~1.5 m).

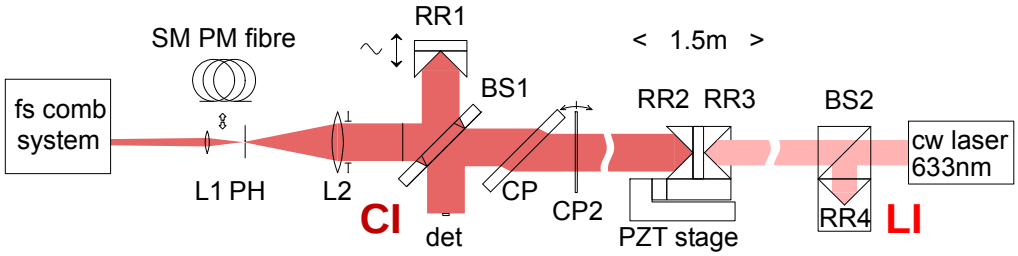

Fig. 6. Setup used for comparison of comb interferometer (CI) and counting laser interferometer (LI).

The beam of the femtosecond laser is expanded and collimated by a spatial filter (lenses L1 and L2 have focal lengths of 30 mm and 250 mm, respectively; the diameter of pinhole PH is 50 μm). The incoming beam is split by a beam splitter (BS) with a dielectric 50% mirror (Thorlabs BSW08). The reference beam is reflected by a hollow gold-mirror retroreflector RR1. Its position can be modulated for quick detection of interferograms. The measuring beam passes through dispersion compensating plates (CP) (fixed) and CP2 (adjustable) to the assembly of two retroreflectors, RR2 (hollow, gold) and RR3 (glass), that are firmly attached together. This assembly can be moved by 1.5 m and finely positioned by screw and piezo. The displacement of the stage is measured by a counting interferometer (Renishaw) from the other side for comparison.

#108459 - $15.00 USD Received 10 Mar 2009; revised 17 Apr 2009; accepted 18 Apr 2009; published 19 May 2009

During the comparison between the comb interferometer (CI) and the counting interferometer (LI), the assembly of RR2+RR3 is moved among three positions corresponding to 0, 1, or 2 times l_{pp}, respectively, as determined by the CI. The displacement of these positions is measured by the LI as well.

First, zero delay between RR1 and the RR2+RR3 assembly is set such that interference is observed (maximal fringe contrast—peak of envelope or center of gravity, or other feature of interferogram). At this position the counting interferometer is reset to zero and the interferogram is stored. Subsequently the RR2+RR3 assembly is moved such that a new coherence maximum is found. Again, the interferogram is stored and the LI value is read. The effective group refractive index is calculated by the numerical model described above from measured atmospheric parameters (pressure, temperature, humidity, CO_2 content) and detected pulse spectra (see next section for details about spectra detection).

The reference retro-reflector (EO NT46-181, 12 mm aperture) is put on a piezoelectric transducer (membrane Piezo-speaker) being in resonance (~200 Hz). This allows for modulation by hundreds of fringes with low voltage (±8.25 μm with ±1 V; the dependence of mechanical amplitude on AC voltage amplitude is linear up to ±66 μm/±8V). The increasing amplitude of modulation brings higher requirements for detector speed (because of increasing number of fringes detected in one modulation period). It is advisable to check the detector speed and effect of transducer tilts with a single mode cw laser; the detected fringe amplitude should not change during the modulation period. Another test is that when blocking any of the arms there should be no residual amplitude modulation. A TiePie Handyscope HS3 (USB AD converter) is used for modulation waveform generation and signal detection. In resonance the transducer movement is pure harmonic (hysteresis is negligible) and the position/time dependence could be easily linearized by recalculating the time to position (similar to an XY oscilloscope with an adjustable phase delay). The overlapping of back and forth traces is better than 40 nm (fringe/10 or the amplitude/200) for standard ±1V modulation.

Besides spectral filtering, the alternative way of detecting a high contrast signal even for high dispersion (long distances) is to observe the interferometer output directly by a spectrometer [10], but vibrations and turbulences comparable to wavelength or higher within the spectrometer integration time would erase the spectral modulation. So we propose to use the spectral filter for obtaining a high-contrast interference signal by a fast detector and to use this signal for locking the path difference to the light or dark fringe (or to the edge) and then observing the (now static) spectral modulation by spectrometer. It was done experimentally, but currently only for short distances. A variant of such spectrally resolved phase detection, but by direct Fourier spectrometry instead of using a separate grating spectrometer, is described at the end of the next section.

6. Experimental results

The interferogram was detected for the path length differences of 0, l_{pp}, and $2l_{pp}$. Before the first comparison of CI and LI we measured the comb spectra with a solid-state spectrometer (Ocean Optics). However, during the evaluation of the comparison of the distance measurement between the frequency comb and the laser interferometer, we found a systematic deviation of CI–LI approximately -4×10^{-7} in relative (about one fringe per meter). Such a large deviation could not be explained by alignment (the cosine error is below 2nm/m) or LI deviation (calibrated and corrected to below 50nm/m) or spectrometer error (a central wavelength error of 15 nm would explain it, but the spectrometer uncertainty was better than 2 nm). As we were not able to identify other possible sources of error, we decided to evaluate what is the real detected spectrum of the detected (linearized) interferogram by Fourier analysis. The sensitivity of the piezo modulation was calibrated by aligning an auxiliary single-mode 633 nm laser alternately to comb radiation. It was found that sensitivity varies with time, temperature, amplitude, frequency, and DC bias, but day-to-day reproducibility is about 0.5% (4 nm/800 nm). This may be acceptable because the related contribution to relative uncertainty of distance measurement is 7×10^{-8}, or it can be improved by more frequent calibration.

#108459 - $15.00 USD Received 10 Mar 2009; revised 17 Apr 2009; accepted 18 Apr 2009; published 19 May 2009

The result of Fourier analysis shows that the spectrum detected by the interferometer significantly deviates from that measured by the spectrometer (Fig. 7). Short wavelengths are suppressed, which is opposite to the spectral sensitivity given by the photodiode manufacturer. The reason for this discrepancy is probably the lack of spectral sensitivity calibration of the spectrometer. The spectral sensitivity of a CCD array substantially differs from that of photodiode. At 800 nm a typical CCD is more sensitive at shorter wavelengths (about -60% per 100 nm), whereas a Si photodiode is more sensitive at longer wavelengths (10% per 100 nm).

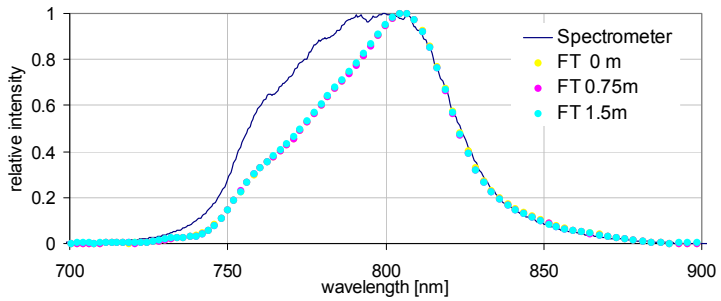

Fig. 7. Comparison of the spectra detected by a spectrometer (solid curve) and calculated by Fourier analysis of an interferogram (dots). The difference between spectra leads to a relative deviation of mean group refractive indices of 1.01×10^{-7}.

However, absolute calibration of spectral sensitivity is not important here; only the relative strength of spectral components actually detected in interferogram is important. If the mean group refractive index is evaluated for the spectrum actually detected by the interferometer, the relative agreement between LI and CI is better than 5×10^{-8}. This is illustrated in Fig. 8, which shows the relative difference between LI and CI for various measurements.

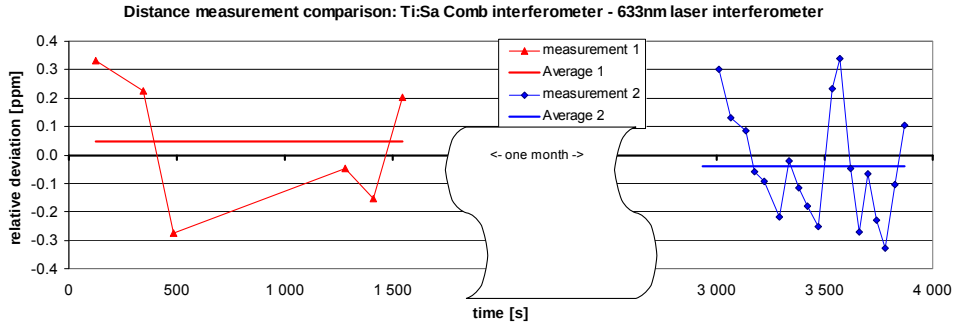

Fig. 8. Result of comparison of comb interferometer and classical counting interferometer for 1.5 m distance/displacement measurement.

The previously mentioned deviation of 4×10^{-7} rel. was caused by the combination of spectral sensitivity of the interferometer and the real change of spectra due to a drift of the fs comb laser after measurement with the spectrometer. The possible instability of fs laser spectra only emphasizes the value of real-time evaluation of spectra from the interferogram, which is by the way easier and directly traceable as compared with the complicated traceable calibration of a spectrometer (wavelength and sensitivity) and a photodiode of an interferometer detector (reflectance of mirrors and beam splitter are not important when measuring the spectra at the interferometer output). Here only the calibration of the amplitude of piezoelectric transducer modulation by counting the number of fringes with a calibrated cw laser is sufficient for a correct evaluation of the actual detected spectral shape (defining actual effective group refractive index).

#108459 - $15.00 USD Received 10 Mar 2009; revised 17 Apr 2009; accepted 18 Apr 2009; published 19 May 2009

The scatter of 3×10^{-7} rel. as shown in Fig. 8 is solely due to the instability of laboratory conditions (the temporal inhomogeneity between LI and CI paths) and not by the resolution and reproducibility of the interferogram detection, which was about 10 times better. For each point both CI and LI values were corrected to actual atmospheric conditions.

The detected spectrum obtained by Fourier analysis of the interferogram cannot only be used to evaluate the mean group refractive index, but also can be used for modeling the shape of the corresponding interferogram at any distance. The spectrum is obtained from the interferogram at zero delay and used to calculate the interferogram at a delay at any distance. This leads to good agreement between calculated and measured interferograms. Since the dispersion that is common to both interferometer arms does not influence the shape of the first-order interferogram, we also used a 10 m standard single-mode polarization-maintaining fiber to deliver the beam from the comb laser to the interferometer. Due to dispersion in the fiber the pulses are extended from few micrometers to millimeter length, and the second-order interferogram is not detectable anymore due to low peak power. However, the linear interferogram remains a few microns long (FWHM ~10 fringes) for zero and 1.5 m distance and the contrast remains close to 100%. This is shown in Fig. 9.

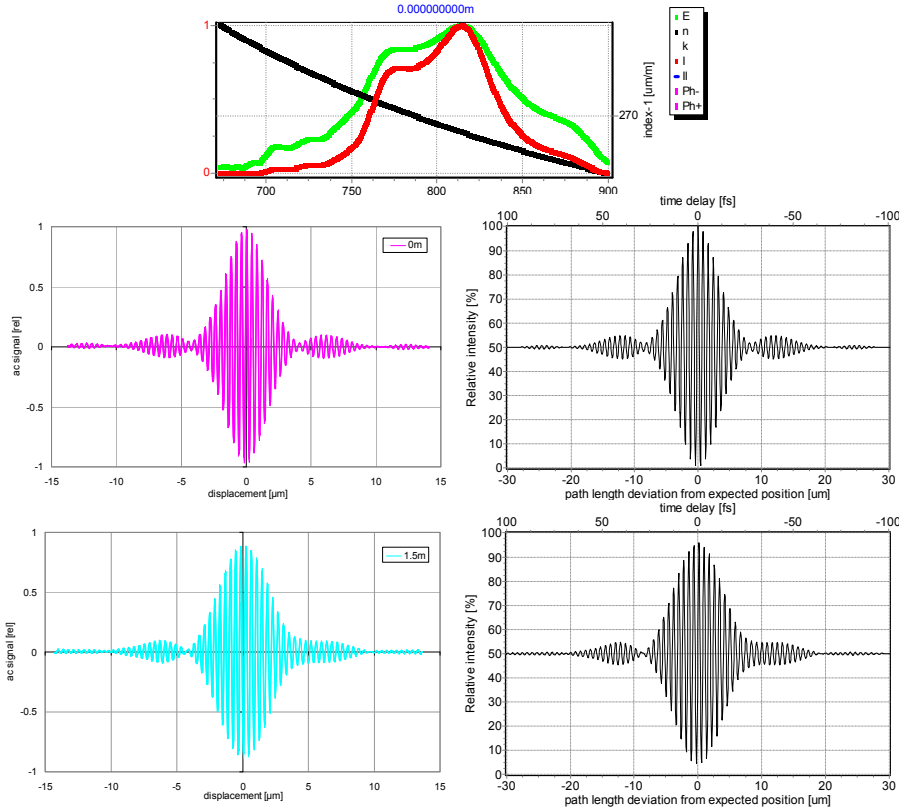

Fig. 9. Illustration of good agreement between detected interferogram and modeled shapes and of envelope development with increasing distance traveled in air. Top, spectra calculated from top left interferogram and used for modeling. Experimental profiles are left and modeled right. Top pair of profiles for zero arm difference, bottom pair for 1.5 m distance ($2*l_{pp}$).

Fiber delivery of the pulse to the interferometer is useful for possible practical applications. Minoshima *et al.* also used the fiber connection between an Er: fiber fs comb laser and the distance measuring equipment [9]. But their method is based on phase measurement at 200 multiple of a repetition rate 50 MHz (i.e. 15 mm wavelength) and not on optical phase measurement.

#108459 - $15.00 USD Received 10 Mar 2009; revised 17 Apr 2009; accepted 18 Apr 2009; published 19 May 2009

A good agreement between the model and the experiment is also observed if the second harmonic is copropagating with the fundamental wavelength (in this case fiber was not used). After propagation through 3 meters of air, the near-IR and blue pulses are completely separated (see Fig. 10 and (Media 1)). Both Fig. 9 and (Media 1) show good agreement between the measured and the calculated interference patterns for different fs laser settings and distances. In Fig. 9 the modeled (black) shapes are calculated using only amplitude spectral information from the Fourier transform of a measured zero interferogram, i.e., supposing a perfect dispersion compensation between interferometer arms in the position of zero interferogram (phase information of FT is not used, see later text). In (Media 1) both amplitude and phase information from the zero interferogram FT are use for the model, because arm dispersion compensation is relatively worse for a broad spectral range.

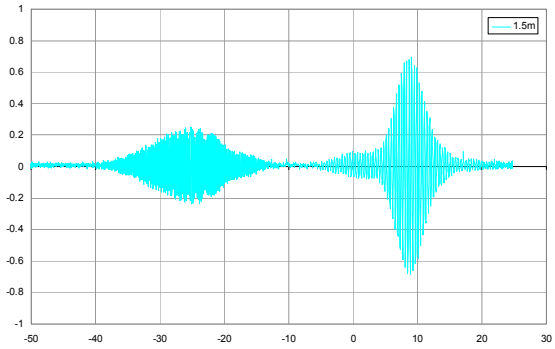

Fig. 10. Separation of NIR and blue (SHG fro NIR) parts of originally overlapping pulses by different group velocities for 3 m path in air (1.5 m distance). Spectra and fringe resolved pictures of measured and modeled interferograms are shown in (Media 1).

To improve repeatability of measurement of l_{pp}, we have changed the arrangement so that both CL and LI measure the same distances between common retro reflectors and beam splitter, so the drift influence is suppressed because values of LI and CI are taken the same time. During this test we use narrow beams (diameter ~2mm), which are spatially separated next to common axis. The comb radiation is again delivered via fiber (angle polished with attached lens collimators). When observing interferogram position by eye, the repeatability is not improved much; a scatter of up to 1/3 of the fringe is mostly due to residual amplitude noise and is also affected by the less than perfect coincidence of sampling and fringe peaks. When evaluating interferogram positions by computer, e.g., as the center of gravity of the absolute value of an ac signal or as the center of gravity of the squares of an ac signal, the measured distance between consecutive interferograms is repeatable to better than ±20nm/1.5m (±13.10^{-9}rel). However, a systematic deviation of about 100nm/1.5m was found. The reason is that the center of gravity of a square of the electric field of the reference arm pulse does not coincide exactly with the center of gravity of the interferogram (light intensity produced by interference of reference and measuring arm E-field pulses) when real (asymmetric) spectra or a less than perfect dispersion compensation of arms is used (the model and measurement agree).

It means that l_{pp} defined by a distance of the centers of gravity is not good enough to reach 0.1 ppm relative uncertainty at a short distance in the case of a non-perfect or not perfectly known compensation of dispersion between the arms. But, it should be noted that the above mentioned problem of the center of gravity ambiguity is, in our case, only 1/8 of the fringe or 1% of FWHM of the detected interferogram. For long-distance and optimal spectral filtering, when whole interferogram length is about 0.1 ppm of the distance to be measured (see Table 1), minor differences between different ways of interferogram center evaluation should not be a problem.

One solution for precise measurement of a short distance would be to take the amplitude and phase information from the zero interferogram (i.e., modeling exactly the profile that was

#108459 - $15.00 USD Received 10 Mar 2009; revised 17 Apr 2009; accepted 18 Apr 2009; published 19 May 2009

detected and taking the residual of the arms dispersion into the model) and then to model its propagation and use it for prediction of the selected property (peak of envelope, center of gravity, peak of highest fringe, or any other) at the distance to be measured.

However, when accepting the need to do a Fourier transform and to use the phase information, it is easier to evaluate directly the position of a stationary phase point for each interferogram, e.g., the position at which the phase does not depend on wavelength (frequency) where $\partial\varphi(\lambda)/\partial\lambda=0$ (see the "center" of phase modulation in Fig. 4). This position Δx can be estimated as

$$\Delta x(\lambda) = \frac{\partial\varphi(\lambda, x_0)}{\partial\lambda} \cdot \frac{\lambda^2}{2\pi} \cdot \tag{7}$$

Δx is the distance from the position x_0 at which the Fourier transform with phases $\varphi(\lambda,x_0)$ was calculated, and also where the value of the reference laser interferometer was read. When we added the difference of Δx for the zero and $1*l_{pp}$ interferograms to the distance measured by LI, we got better agreement with the predicted l_{pp} than in case of the center of gravity evaluation. Using the distance between the next stationary phase points for a certain wavelength means that only the simple group refractive index at that wavelength is needed. That is, no weighting to the effective group refractive index is needed.

The results of this method of evaluation are shown in Fig. 11 for three wavelengths, 790 nm, 800 nm and 810 nm, and for seven slightly different arrangements (beam alignments, beam collimations, with/without compensating plate CP2, with/without 800 μm aperture in front of a 2 mm photodiode detector).

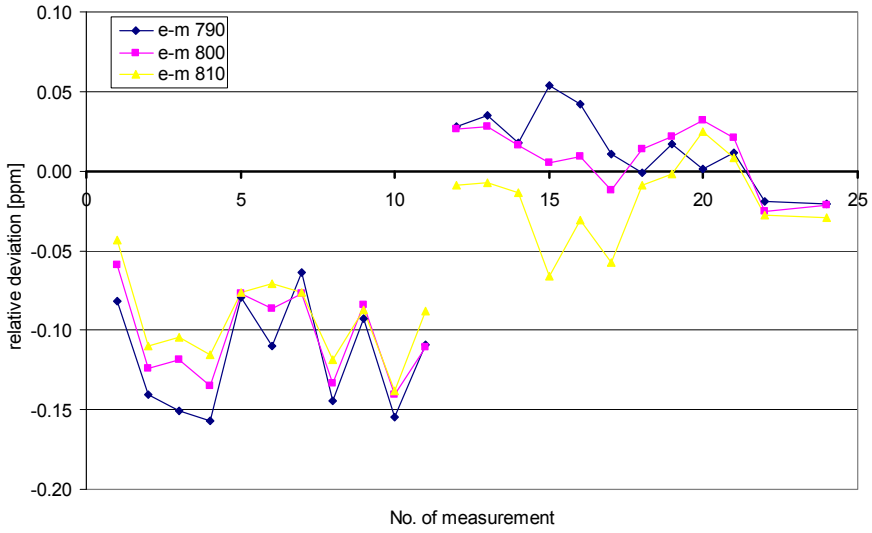

Fig. 11. Results of CI–LI comparison for evaluating stationary phase points for three different wavelengths. Effectively it means the direct measurement of group refractive indices at these wavelengths by laser interferometer LI. The deviation of experimentally measured group refractive index (or of $l_{pp}(\lambda)$) from the calculated by Ciddor formula is shown. The systematic deviation of results 1–11 was caused by wrong comb beam collimation.

The systematic deviation in the first half of Fig. 11 (numbers 1 to 11) is mainly due to an imperfect collimation of the comb beam coming from the fiber (the collimator works well for 633 nm but is not achromatic; the chromatic error makes the beam at 800 nm diverge about mm per m, which could make a cosine error of up to 0.5 ppm, but averaging across photodiode area makes the error about 0.1 ppm). In the second part of Fig. 11 the additional lens was used to collimate the radiation around 800 nm. The agreement between the calculated and experimentally evaluated $l_{pp}(\lambda)$ or $n_g(\lambda)$ is better than 0.1 ppm for each wavelength used. The relative deviation of l_{pp}(790 nm) and l_{pp}(810 nm) is 0.36 ppm.

#108459 - $15.00 USD Received 10 Mar 2009; revised 17 Apr 2009; accepted 18 Apr 2009; published 19 May 2009

We suppose that residual deviations come from a chromatic error of two kinds. First, there is the chromatic error of collimator and different diffraction of different wavelengths; it can be improved to some extent by using a larger beam diameter, collimating the radiation outputting the fiber with a parabolic mirror only (without lens), and by detecting only the central part of the beam profiles. Second, the beam splitter mirror is deposited on the wedged glass (Thorlabs BSW08, 30' wedge), so the transmitted beam is spectrally divided as if by an optical prism. But this division is small—a 30' wedge from BK7 tilts the beam entering at 45° by 7.836 mrad for 852.1 nm wavelength and by 7.880 mrad for 706.5 nm wavelength. The difference of 44 μrad brings a cosine error of only 1.10^{-8}rel. and it is further compensated by a compensating plate CP (Thorlabs BSW08-1-OC, also 30') placed anti-parallel behind the beam splitter.

The above described experiment is in fact a variant of a direct measurement of the group refractive index of air. Yamaoka *et al.* used a gauge block as a reference [15] and got scatter and agreement to the Edlen formula to 2.10^{-7} rel. (standard deviation). We use a 633 nm interferometer with a phase refractive index calculated by the Ciddor formula as a reference. We got both scatter and agreement of measured and calculated group refractive indices of better than 1.10^{-7} rel. (two standard deviations) in this preliminary arrangement.

7. Conclusion

We have developed a powerful numerical model of pulse propagation in air. It can be used for the calculation of the effective group refractive index of any visible or near-infrared spectra and for prediction of interferogram shapes at any distance. The optimal spectral widths for long-distance measurement with violet, red, and infrared frequency comb radiation have been calculated. It was shown that long-distance measurement in air with frequency comb radiation is possible and is advantageous, especially for infrared (e.g. ~1550 nm) combs. The fast scanning detector enables clear resolution of interference fringes in conditions where they would be deformed or suppressed by vibrations, turbulences, or wavelength instability for longer integration times. The comparison with a counting interferometer proves that the distance calculated with a modeled group refractive index agrees with experiments to 5×10^{-8} on average if calculation is done for actually detected spectra. Alternative methods of evaluation using phase information from a Fourier transform is proposed and demonstrated. It could lead to precise measurement of dispersion/group refractive indices after an improvement of the experimental arrangement. It was demonstrated that first-order interferograms remain transform limited, even if highly chirped and elongated pulses enter the interferometer, allowing for delivering the frequency comb radiation to the interferometer by an optical fiber.

Acknowledgments

The international project Absolute Long-distance Measurement in Air is part of the European Metrology Research Programme (EMRP) http://www.emrponline.eu/selected-JRPs.html [16]. The research within this EURAMET joint research project leading to these results has received funding from the European Community's Seventh Framework Programme, ERA-NET Plus, under grant agreement 217257. The Ministry of Industry and Trade of the Czech Republic partially supported this work in project FT-TA3/133. We thank the partners of the Long Distance project, especially the coordinator J.-P. Wallerand, and Massimo Zucco for discussions and comparison of model results.

#108459 - $15.00 USD Received 10 Mar 2009; revised 17 Apr 2009; accepted 18 Apr 2009; published 19 May 2009